Engineering and Applied Sciences
2024, Vol. 9, No. 4, pp. 53-62
https://doi.org/10.11648/j.eas.20240904.11

Review Article

Application of 2-D Molybdenum Disulfide in the Field of Photoelectric Detection

Xiaochen Sun, Jiaying Jian*, Zengyun Jian

School of Materials and Chemical Engineering, Xi'an Technological University, Xi'an, China

Abstract

The research of photodetectors is rooted in the principle of photoelectric effect, which has become indispensable in human society. Photodetectors convert light signals into electrical signals and represent a crucial subdivision within modern optoelectronic technology. They play significant roles in optical communications, remote sensing, biomedical applications, industrial automation, and more. Two-dimensional MoS_2 has attracted considerable attention in optoelectronics due to its unique structure and performance characteristics. The research methods for photodetectors primarily include: Material Selection: Using semiconductor materials such as silicon, germanium, gallium arsenide, and indium arsenide. Silicon, in particular, is widely applied in optical communications, computer networks, medical diagnostics, and more. Technological Improvements: This involves high sensitivity detection techniques, automatic alignment technologies, and composite integration techniques to enhance the performance and application domains of photodetectors. Application Development: Exploring new applications of photodetectors in optical communications, medical imaging, security monitoring, etc., and improving their reliability and efficiency in practical applications.Research on photodetectors not only enhances their efficiency and performance in fields like communication, medicine, and security monitoring but also lays a solid foundation for future technological innovation and application expansion. With continuous advancements in technology, photodetectors are demonstrating vast application prospects and substantial market potential. Finally, the prospects and challenges associated with photodetectors in practical applications are also discussed.

Keywords

Two-Dimensional MoS_2, Photodetectors, Photoelectric Performances

1. Introduction

Photodetectors (PDs) have a wide range of applications in various fields such as industrial, defense, military, environmental monitoring, and biology [1-8]. To advance the development of high-performance PDs, researchers are exploring two-dimensional (2D) semiconductor materials, focusing particularly on 2D transition metal dichalcogenides (TMDs) such as MoS_2, WS_2, $MoSe_2$, WSe_2, $MoTe_2$, and WTe_2, due to their unique electronic, optical, magnetic, and thermal properties [9-15]. These materials offer a versatile platform for designing advanced PDs that can overcome limitations of traditional PDs, including complex preparation processes and low-temperature operation [3, 11].

Among TMDs, molybdenum disulfide (MoS_2) stands out as a representative material with distinct physical, optical, and

*Corresponding author: jianjiaying@xatu.edu.cn (Jiaying Jian)

Received: 22 January 2024; **Accepted:** 7 August 2024; **Published:** 27 August 2024

electrical properties, making it a promising candidate for next-generation PDs [16-20]. MoS_2 features a 'three-layer' structure (S-Mo-S), where S layers sandwich Mo layers. This structure is characterized by strong covalent or ionic bonds within layers, with weaker bonding forces between layers [21-23]. MoS_2 exhibits an intrinsic and tunable bandgap, along with relatively high carrier mobility, surpassing graphene in its potential for PD applications [24-26]. In bulk form, MoS_2 is an indirect-gap semiconductor with a bandgap of 1.2 eV, whereas single-layer MoS_2 transitions to a direct-gap semiconductor with a bandgap of 1.8 eV due to quantum confinement [27]. Monolayer MoS_2 demonstrates a single-layer mobility of 200 $cm^2 V^{-1} s^{-1}$, increasing to 500 $cm^2 V^{-1} s^{-1}$ for few layers, highlighting its attractiveness for high-performance optoelectronic devices [25, 28].

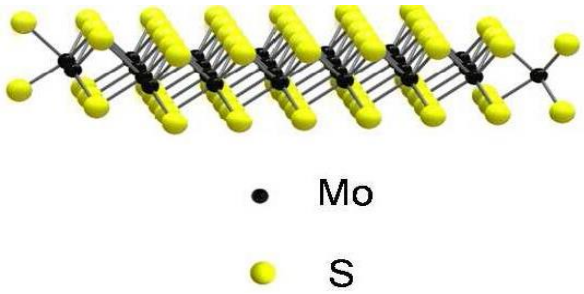

Figure 1. *Molecular structure of MoS_2 [21].*

Despite facing challenges such as low light absorptivity and higher dark current, MoS_2-based PDs can overcome these limitations by integrating with other semiconductors. The dangling bonds on the free surface of 2D materials facilitate their integration into mixed-dimensional van der Waals heterostructures. This approach combines the unique advantages of 2D materials with those of different dimensional materials, effectively addressing the drawbacks mentioned and expanding the application potential of photodetection.

2. Preparation Method of Molybdenum Disulfide

Fabricating high-performance photodetectors requires producing highly crystalline and top-quality molybdenum disulfide (MoS_2). Common methods include scotch tape-based micromechanical exfoliation [16, 24], intercalation-assisted exfoliation [29-31], liquid exfoliation [32], physical vapor deposition [33, 34], hydrothermal synthesis [35], and chemical vapor deposition [36, 37]. Feng et al. [38] employed a solvothermal approach to fabricate MoS2 nanosheets, achieving an average size of approximately 90 nm with thickness ranging from 10 to 20 nm. Ji et al. utilized liquid exfoliation to prepare two-dimensional MoS_2 nanosheets [39], resulting in nanosheets with lateral sizes in the range of a few micrometers and thicknesses varying from approximately 1 to 10 nm.

Currently, research on photoelectric detection equipment predominantly utilizes the mechanical exfoliation method [40-45]. This method involves using scotch tape to peel single and multi-layer MoS_2 films from bulk MoS_2, which are subsequently deposited onto Si/SiO_2 substrates. Qiao et al. successfully synthesized large-area, high crystalline quality vertically few-layered MoS_2 (V-MoS_2) nanosheets using the chemical vapor deposition (CVD) technique. These nanosheets were grown on a Si/SiO_2 (300 nm) substrate, as shown in Figure 2a and 2b [46]. The V-MoS_2 structure consisted of vertically layered nanosheets with an average thickness of approximately 3 nm (equivalent to 4 layers of MoS_2) and a height of about 2 μm.

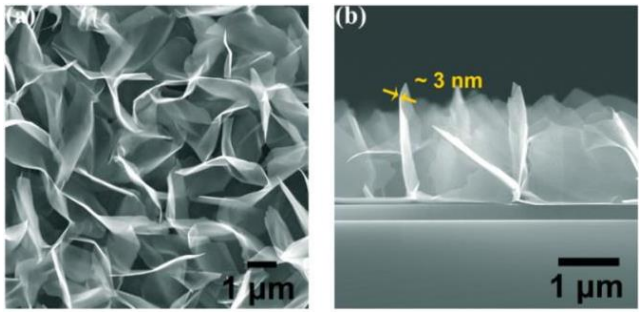

Figure 2. *From the top to the bottom, and (b) Cross-sectional SEM images of V-MoS_2. [46].*

Additionally, Pak et al. fabricated monolayer MoS_2 using CVD, grown on a SiO_2 (300 nm)/Si substrate. The morphology of the monolayer MoS_2 was triangular, with a thickness measured at approximately 0.7 nm, as depicted in Figure 3(a) and (b) inset [47].

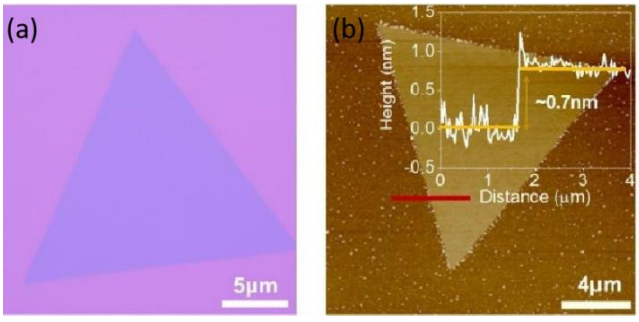

Figure 3. *Optical image (a) and AFM topography image (b) of monolayer MoS_2 [47].*

3. Wavelength Detection Range of MoS_2 and Its Heterojunctions PDs

MoS_2 and its heterojunction photodetectors demonstrate broad waveband detection capabilities spanning from ultra-

violet to infrared. For instance, the MoS_2/CdTe p-n heterojunction photodetector exhibits a broadband spectrum response from 200 nm up to 1700 nm [3]. Similarly, the vertical multilayered MoS_2/Si homojunction photodetector shows a wide detection spectrum from visible to near-infrared [48]. Additionally, the MoS_2/Black phosphorus heterojunction photodetector covers the visible to mid-infrared spectral range [49]. Moreover, the MoS_2/GaAs heterojunction photodetector offers a broad response spectrum from deep ultraviolet (DUV) to near-infrared (NIR) [50]. Furthermore, a few-layer MoS_2 Schottky photodetector with back-to-back MSM geometry enables broadband photodetection from the visible to UV regions [51]. Lastly, the vertical layered MoS_2/Si heterojunction photodetector exhibits a wide photoresponse ranging from 350 to 1100 nm [46].

4. Photocurrent Generation Mechanism

The main mechanisms of photocurrent generation including photovoltaic effect, photoc-onductive effect and photothermoelectric effect.

4.1. Photovoltaic Effect

In the photovoltaic (PV) effect, a semiconductor PN junction generates electron-hole (e-h) pairs upon absorbing incident photons with sufficient energy. When the optoelectronic device is illuminated without external voltage, these photogenerated e-h pairs can be separated by the built-in electric field originating from either a p-n junction or a Schottky junction at the interface between the semiconductor and metal contact. The separated charges flow in opposite directions through the junction area, thereby generating photocurrent in the external circuit [52-56]. The internal electric field is established at the Schottky barrier or PN junction interface, as illustrated in Figure 4(a). Figure 4(b) depicts the I-V characteristics of the PN junction under illumination and in darkness [57].

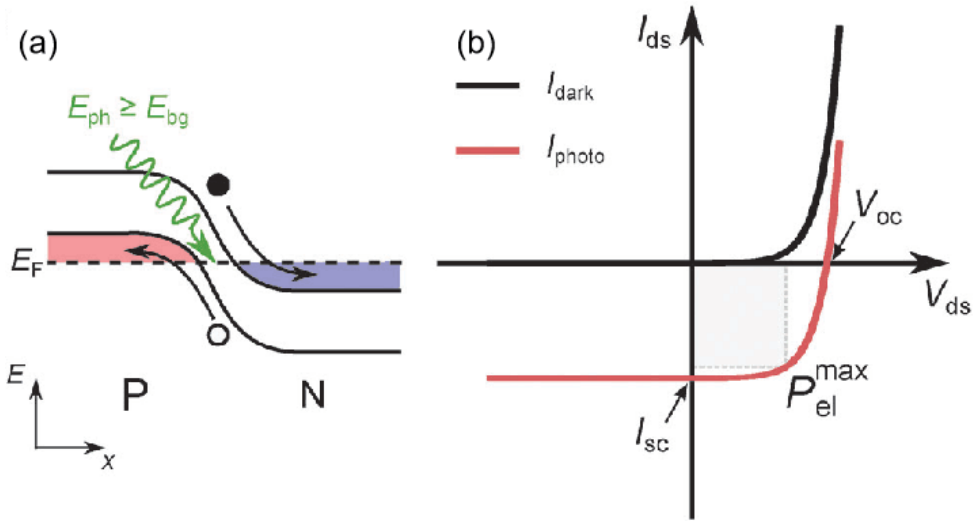

Figure 4. *Schematic diagram of the photovoltaic effect. (a) Band alignment in a PN junction. (b) I-V curves in the dark and under illumination [57].*

4.2. Photoconductive Effect

In the photoconductive effect, incident light radiation energizes the semiconductor, inducing excess carriers that increase the free carrier concentration and thus reduce the electrical resistance [58-61]. These excess carriers are separated under an applied bias voltage, generating photocurrent as a result [62-65]. In the absence of light, a small dark current flows between the two electrodes (Figure 5(a)). When the device is illuminated, photons with energy (E_{ph}) higher than the bandgap (E_{bg}) create electron-hole pairs that are then separated by the applied voltage (Figure 5(b)) [57].

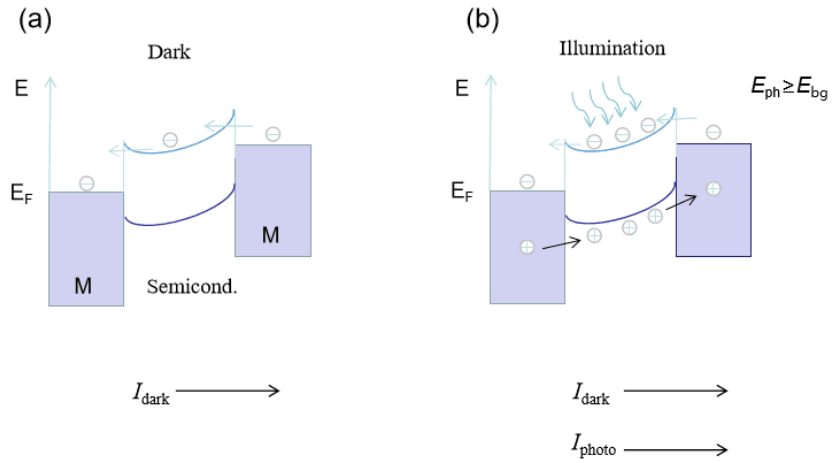

Figure 5. *Schematic diagram of the photoconductive effect. (a) without illumination. (b) Under illumination [57].*

4.3. Photothermoelectric Effect

The photothermoelectric effect (PTE) is a thermal phenomenon induced by light irradiation [66-69]. When the detector absorbs light radiation energy, the smaller spot of light compared to the size of the device channel causes a change in the semiconductor's temperature, resulting in a temperature gradient across the semiconductor channel [70-72]. Figure 6 [57] illustrates different temperature differentials (ΔT) at the two ends of the semiconductor channel. Utilizing the Seebeck effect, this ΔT can be converted into a voltage difference (ΔV). According to the Seebeck coefficient (S), the magnitude of ΔV is linearly proportional to the temperature gradient:

$$\Delta V = S \cdot \Delta T \quad (1)$$

For example, a steady-state ΔT was kept • between two junctions by a focused illumination on the electrical contacts, leding to a voltage difference (ΔV_{PTE}):

$$\Delta V_{PTE} = (S_{semiconductor} - S_{metal}) \cdot \Delta T \approx S_{semiconductor} \cdot \Delta T \quad (2)$$

Usually, the magnitude of VPTE often ranges from tens of μV to tens of mV. Therefore, a high-quality Ohmic contact of the metal and semiconductor contacts is required.

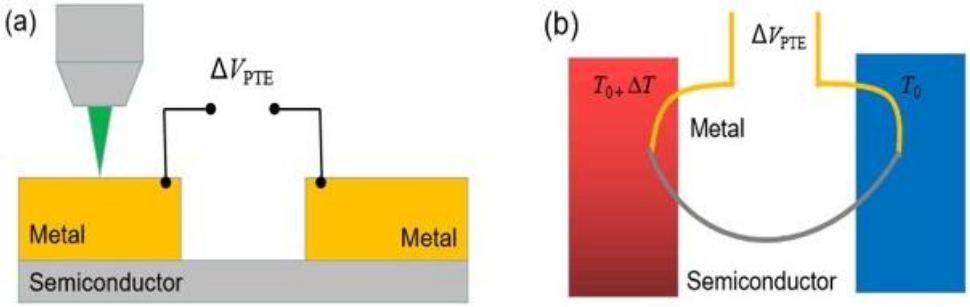

Figure 6. *Schematic diagram of the photo-thermoelectric effect. (a) Schematic of a field-effect transistor. (b) Thermal circuit corresponding to the device depicted in (a) [57].*

5. Performance Parameters of Photodetector

5.1. Photoresponsivity (R)

$$R_I = I_{Ph} / P \quad (3)$$

where IPh is the photocurrent, P is the incident light power, which is one of the main performance indexes of photoelectric detectors.

Photoresponsivity is explained as the ratio of the photocurrent to the incident light power, that is, the ratio of output electric signal current size to input optical signal power size, expressed as:

The MoS_2/CdSe hybrid phototransistor was designed by

Ra et al. [73], which exhibited excellent photodetector performances, such as the responsivity of the device was 2.5×10^5 A/W, MoS_2/CdSe phototransistor schematic diagram was shown from figure 7.

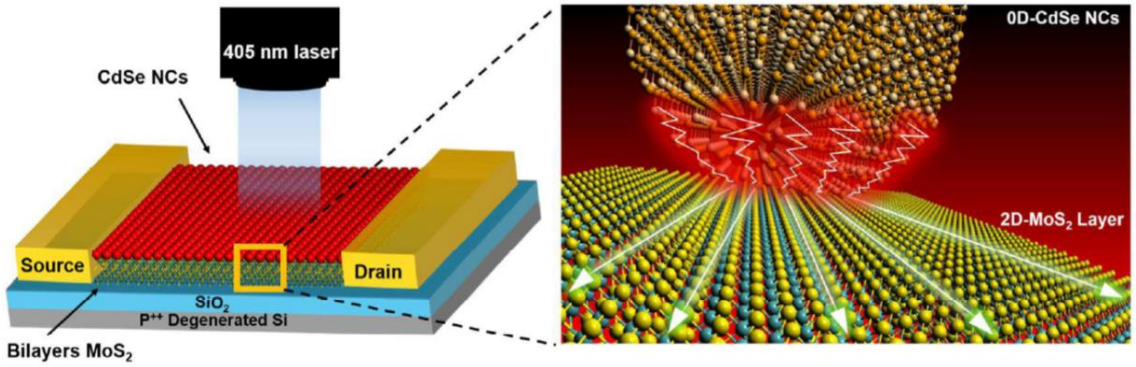

Figure 7. *MoS_2/CdSe phototransistor [73].*

The MoS_2/PbS quantum dot photodetector was made by Kufer et al. [74], which showed dramatically higher responsivity of $6\times10^5 AW^{-1}$, the photodetector architecture was illustrated in Figure 8a with a cross sectional view of the photoelectric detection device operation in Figure 8b.

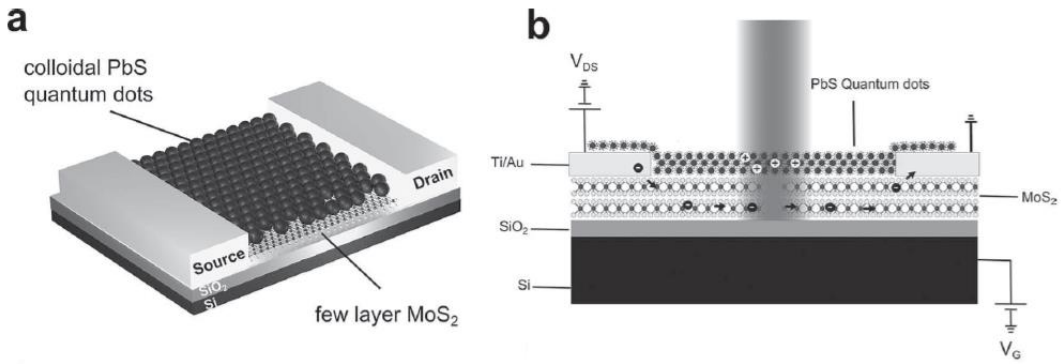

Figure 8. *a 3D view and b Cross sectional view of MoS_2/PbS quantum dot photodetector [74].*

Few-layer MoS_2 lied above monolayer molybdenum MoS_2 of a sensitized MoS_2 phototransistor was fabricated by Yang et al. [75], which exhibited an ultrahigh responsivity of ~105-106 AW-1 (at zero and positive Vg) due to the special construction of MoS_2 phototransistor (the schematic of MoS_2 phototransistor from top and side views was shown in Figure 9a and b, respectively,), thus the photon absorption and higher mobility enhanced.

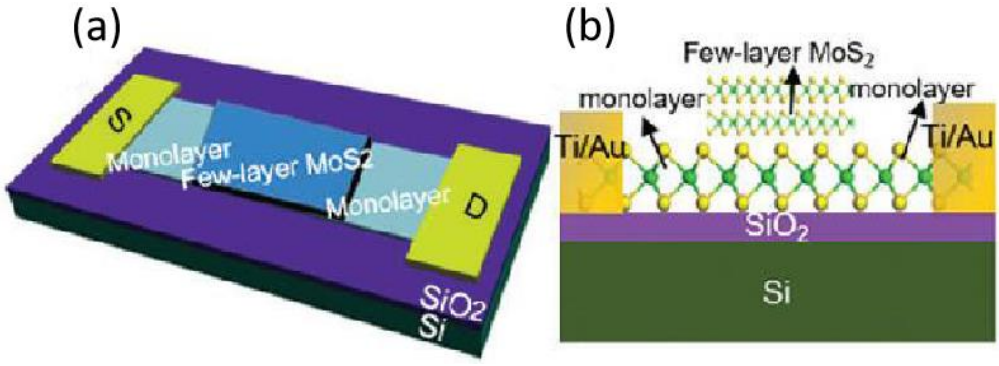

Figure 9. *(a) Top view and (b) side view of the MoS_2 phototransistor schematic diagram [75].*

5.2. Normalized Detectivity (D*)

Normalized Detectivity is also one of the main performance indexes to characterize the sensitivity of photoelectric detectors, which represents the sensitivity of photoelectric detectors, Normalized detectivity is expressed as:

$$D^* = \frac{\sqrt{AB}}{i_N} R \tag{4}$$

where A is the area of detectrs, B is the bandwidth, i_N is the noise current spectra at 1 Hz bandwidth with units of A $Hz^{-1/2}$, R is the Photoresponsivity, the D* is measured in cm $Hz^{1/2}$ W^{-1} (Jones) [76]. The detectivity of the MoS_2/CdSe hybrid phototransistor was 1.24×10^{14} Jones, the device was designed by Ra et al. [73]. Monolayer MoS_2/GaAs heterostructure self-driven photodetector was fabricated by Xu et al. with the detectivity of 1.9×10^{14}Jones [77]. Kufer et al. made the MoS_2/PbS photodetector with extremely high detectivity of 5×10^{14}Jones [74].

5.3. Response Speed

The response speed is also one of the key parameters of the photodetectors, a short response time represents a fast response speed, which reflects the sensitivity, ensuring a varied optical signal can be significantly followed [78-80]. In the time domain, the response speed of PDs is usually characterized by the rise time (τ_r, the time interval of the maximum photocurrent from 10% to 90%) and the fall time (τ_f, the time interval of the maximum photocurrent from 90% to 10%) of the steady-state photocurrent. [48, 81-83]. When the PDs is exposed to different wavelengths of light, the incident light is absorbed will result in the generation of electron-hole pairs, which will be quickly separated by the strong built-in electric field in p-n junction or different doping interval and then transferred to the electrodes, leading to an increase in photocurrent and a fast response speed. Near-infrared photodetector based on MoS_2/black phosphorus heterojunction was manufactured by Ye et al. with a fast response speed, the response was characterized by a typical rise time of τ_r=15 μs and τ_f=70 μs [49]. The V-MoS_2/Si heterojunction photodetector was composited by Qiao et al. [46], because of the special vertical structure of the photodetector was illustrated in Figure 10, which demonstrated excellent photoelectric property, particularly an ultrahigh response speed (rise time ~ 56 ns, fall time ~ 825 ns) by time response measurements, which is the fastest response speed achieved at present in different 2D-based photodetectors.

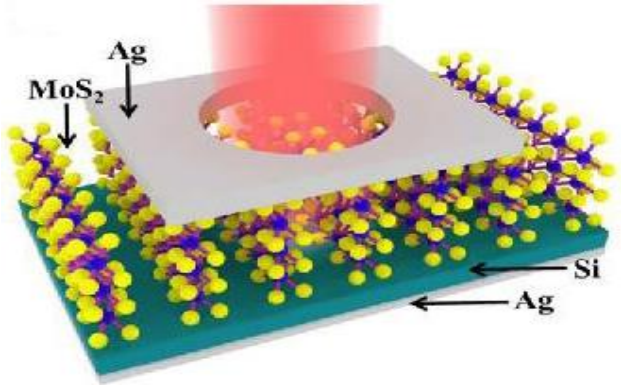

Figure 10. *Schematic illustration of the V-MoS_2/Si heterojunction PD [46].*

Table 1. *Performance of 2-D MoS_2 and its heterojunctions devices.*

Materials	R (A W^{-1})	Response speed	D*(Jones)	Ref
MoS_2	~10^5-10^6	–	9.3×10^{12}	[75]
MoS_2	880	4/9s	–	[27]
MoS_2	0.57	70/110μs	~10^{10}	[51]
MoS_2/p-Si	908.2 mA/W	56/ 825 ns	1.889×10^{13}	[46]
MoS_2 /n-Si	11.9	30.5/71.6μs	2.1×10^{10}	[48]
MoS_2/CdTe	36.6 mA/W	43.7/82.1μs	6.1×10^{10}	[3]
MoS2/CdSe	2.5×10^5	60/60ms	1.24×10^{14}	[77]
MoS_2/GaAs	35.2 mA /W	3.4/15.6ms	1.96×10^{13}	[50]
MoS_2/ZnO-QDs	2267	12 /26s	2.1×10^{11}	[84]
MoS_2/Graphene	10^4mA /W	0.28/1.5s	–	[85]
MoS_2/PbS	6×10^5	–/~0.35s	5×10^{14}	[74]

Materials	R (A W^{-1})	Response speed	D*(Jones)	Ref
MoS_2/GaAs	0.419	17/31μs	1.9×10^{14}	[77]
MoS_2/b-P	22.3	15/70μs	3.1×10^{11}	[49]
MoS_2/b-AsP	0.22	0.54/0.52 ms	9.2×10^{9}	[86]
MoS_2/GaAs	0.43mA /W	1.87/3.53 ms	2.28×10^{11}	[87]
MoS_2/β-Ga_2O_3	2.05mA /W	–	1.21×10^{11}	[88]
MoS_2/$MoTe_2$	0.86	–	~ 10^{11}	[89]
MoS_2/CuPc	~1.98	–/< 0.3 s	$\sim 6.1 \times 10^{10}$	[21]
Graphene/MoS_2/Si	0.6	17/48 ns,	8×10^{12}	[90]
MoS_2/WS_2	2.3	–	–	[91]
MoS_2/Si	≈300mA/W	3/40μs	$\approx 10^{13}$	[92]

6. Conclusion and Prospect

In this review, recent state-of-the-art photodetectors based on 2D layered MoS_2 and their heterostructures have been introduced. This photodetectors have a promising prospect in the field of detection and application due to excellent photoelectric performances in broadband spectrum detection, ultrahigh photoresponsivity, fast response speed and higher normalized detectivity.

In recent years, 2D layered MoS_2 based photodetectors rapid development has been achieved. Despite the many advantages mentioned above, MoS_2 based photodetectors with many problems are faced and still have much development ahead for practical applications. 2D materials tend to have a low absorption of light due to their thickness, how to work stably and efficiently for a long time is also a problem for 2D semiconductor optoelectronic devices. In order to realize high-performance 2D photoelectric detector and meet various practical needs, efforts can be made from the following aspects in the future: preparing 2D materials with high quality, using some optical methods to improve the absorption of 2D materials and doping or modifying 2D materials to improve the performance of the PDs.

Abbreviations

DUV	Deep-Ultraviolet
PDs	Photodetectors
2D	Two-Dimensional
TMDs	Transition Metal Dichalcogenides
MoS_2	Molybdenum Disulphide
NIR	Near-Infrared
PV	Photovoltaic
PTE	Photothermoelectric Effec

Funding

This work is supported by the National Science Foundation of China (Grant No. 62204197).

National Science Foundation of China (Grant No. 62204197), Shaanxi Provincial Department of Education (Grant No. 22JK0408), Shaanxi Provincial Department of Science and Technology (Grant No. 2023KJXX-149), Xi'an Association for Science and Technology (Grant No. 959202313058)

Conflicts of Interest

The authors declare that they have no known competing financial interests or personal relationships that could have appeared to influence the work reported in this paper.

References

[1] Liu Y, Yin J, Wang P, et al. High-Performance, Ultra-broadband, Ultraviolet to Terahertz Photodetectors based on Suspended Carbon Nanotube Films. Acs Appl Mater Interfaces. 2018; 10: 36304-36311.

[2] Sang L, Liao M, Sumiya M. A Comprehensive Review of Semiconductor Ultraviolet Photodetectors: From Thin Film to One-Dimensional Nanostructures. Sensors. 2013; 13: 10482-10518.

[3] Wang Y, Huang X, Wu D, et al. A room-temperature near-infrared photodetector based on a MoS_2/CdTe p-n heterojunction with a broadband response up to 1700 nm. J Mater Chem C. 2018; 6: 4861-4865.

[4] Ye L, Wang P, Luo W, et al. Highly polarization sensitive infrared photodetector based on black phosphorus-on-WSe_2 photogate vertical heterostructure. Nano Energy. 2017; 37: 53-60.

[5] Norton PR, Campbell III JB, Horn SB and Reago DA. Third-generation infrared imagers. Proc Spie 2000; 4130: 226-236.

[6] Yao J, Zheng Z, Yang G. Layered-material WS_2/topological insulator Bi_2Te_3 heterostructure photodetector with ultrahigh responsivity in the range from 370 to 1550 nm. J Mater Chem C. 2016; 4: 7831-7840.

[7] Yao J, Zheng Z, Yang G. All−Layered 2D Optoelectronics: A High−Performance UV-vis-NIR Broadband SnSe Photodetector with Bi_2Te_3 Topological Insulator Electrodes. Adv Functional Mater. 2017; 27: 1701823.

[8] Yao J, Shao J, Wang Y, et al. Ultra-broadband and high response of the Bi_2Te_3-si heterojunction and its application as a photodetector at room temperature in harsh working environments. Nanoscale. 2015; 7: 12535-12541.

[9] Yin Z, Li H, Li H, et al. Single-Layer MoS_2 Phototransistors. ACS Nano. 2012; 6: 74-80.

[10] Mak KF, McGill KL, Park J, et al. The valley Hall effect in MoS_2 transistors. Science. 2014; 344: 1489-1492.

[11] Wu W, Wang L, Li Y, et al. Piezoelectricity of single atomic-layer MoS_2 for energy conversion and piezotronics. Nature. 2014; 514: 470-474.

[12] Rhyee J, Kwon J, Dak P, et al. High-mobility transistors based on largearea and highly crystalline CVD-grown $MoSe_2$ films on insulating substrates. Adv Mater. 2016; 28: 2316-2321.

[13] Zhang Y, Chang TR, Zhou B, et al. Direct observation of the transition from indirect to direct bandgap in atomically thin epitaxial $MoSe_2$. Nat Nanotechnol. 2014; 9: 111-115.

[14] Cheng R, Jiang S, Chen Y, et al. Few-layer molybdenum disulfide transistors and circuits for high-speed flexible electronics. Nat Commun. 2014; 5: 5143-5151.

[15] Barja S, Wickenburg S, Liu Z, et al. Charge density wave order in 1D mirror twin boundaries of single-layer $MoSe_2$. Nat Phys. 2016; 12: 751-756.

[16] Splendiani A, Sun L, Zhang Y, et al. Emerging Photoluminescence in Monolayer MoS_2. Nano Lett. 2010; 10: 1271-1275.

[17] Wang H, Yu L, Lee Y-H, et al. Integrated Circuits Based on Bilayer MoS_2 Transistors. Nano Lett. 2012; 12: 4674-4680.

[18] Wi S, Kim H, Chen M, et al. Enhancement of Photovoltaic Reponse in Multilayer MoS_2 Induced by Plasma Doping. ACS Nano. 2014; 8: 5270-5281.

[19] Lee HS, Min S-W, Park MK, et al. MoS_2 Nanosheets for Top-Gate Nonvolatile Memory Transistor Channel. Small 2012; 8: 3111-3115.

[20] Kim S, Konar A, Hwang W-S, et al. High-mobility and low-power thin-film transistors based on multilayer MoS_2 crystals Nat. Commun. 2012; 3: 1011-1017.

[21] Pak J, Jang J, Cho K, et al. Enhancement of photodetection characteristics of MoS_2 field effect transistors using surface treatment with copper phthalocyanine. Nanoscale. 2015; 7: 18780-18788.

[22] Wang Q, Kalantar-Zadeh K, Kis A, et al. Electronics and opto-electronics of twodimensional transition metal dichalcogenides. Nat Nanotechnol. 2012; 7; 699-712.

[23] Garciahernandez M, Coleman J. Corrigendum: materials science of graphene: a flagship perspective 2D Mater. 2016; 3: 019501.

[24] Mak KF, Lee C, Hone J et al. Atomically Thin MoS_2: A New Direct-Gap Semiconductor. Phys Rev Lett. 2010; 105: 136805-136808.

[25] Radisavljevic B, Radenovic A, Brivio J, et al. Single-Layer MoS_2 Transistors. Nat Nanotechnol. 2011; 6: 147-150.

[26] Podzorov V, Gershenson M, Kloc C, et al. High-Mobility Field-Effect Transistors Based on Transition Metal Dichalcogenides. Appl Phys Lett. 2004; 84 3301-3303.

[27] Lopez-Sanchez O, Lembke D, Kayci M, et al. Ultrasensitive photodetectors based on monolayer MoS_2. Nat Nanotechnol. 2013; 8: 497-501.

[28] Yoon Y, Ganapathi K, Salahuddin S. How Good Can Monolayer MoS_2 Transistors Be. Nano Lett. 2011; 11; 3768-3773.

[29] Ramakrishna Matte HSS, Gomathi A, Manna A K, et al. MoS_2 and WS_2 Analogues of Graphene. Angew Chem Int Ed. 2010; 49: 4059-4062.

[30] Zeng Z, Yin Z, Huang X, et al. Single−Layer Semiconducting Nanosheets: High−Yield Preparation and Device Fabrication. Angew Chem Int Ed. 2011; 50: 11093-11097.

[31] Eda G, Yamaguch H, Voiry D, et al. Photoluminescence from Chemically Exfoliated MoS_2. Nano Lett. 2011; 11: 5111-5116.

[32] Zhou K, Mao N, Wang H, et al. A Mixed-Solvent Strategy for Efficient Exfoliation of Inorganic Graphene Analogues. Angew Chem Int Ed. 2011; 50: 10839-10842.

[33] Helveg S, Lauritsen JV, Lægsgaard E, et al. Atomic-Scale Structure of Single-Layer MoS_2 Nanoclusters. Phys Rev Lett. 2000; 84: 951- 954.

[34] Lauritsen J V, Kibsgaard J, Helveg S, et al. Size-dependent structure of MoS_2 nanocrystals. Nat Nanotechnol. 2007; 2: 53-58.

[35] Peng Y, Meng Z, Zhong C, et al. Hydrothermal Synthesis and Characterization of Single-Molecular-Layer MoS_2 and $MoSe_2$. Chem Lett. 2001; 8: 772-773.

[36] Lee Y, Zhang X, Zhang W, et al. Synthesis of Large-Area MoS_2 Atomic Layers with Chemical Vapor Deposition. Adv Mater. 2012; 24: 2320-2325.

[37] Liu KK, Zhang W, Lee YH, et al. Growth of large-area and highly crystalline MoS_2 thin layers on insulating substrates. Nano Lett. 2012; 12: 1538-1544.

[38] Feng X, Tang Q, Zhou J, et al. Novel mixed-solvothermal synthesis of MoS_2nanosheets with controllable morphologies. Cryst Res Technol. 2013; 48: 363-368.

[39] Ji S, Yang Z, Zhang C, et al. Exfoliated MoS_2 nanosheets as efficient catalysts for nelectrochemical hydrogen evolution. Electrochim Acta. 2013; 109: 269-275.

[40] Lee S, Chu D, Song D, et al. Electrical and photovoltaic properties of residue-free MoS_2 thin films by liquid exfoliation method. Nanotechnology. 2017; 28: 195703.

[41] Ky DLC, Tran Khac BC, Le CT, et al. Friction characteristics of mechanically exfoliated and CVD-grown single-layer MoS_2. Friction. 2017. https://doi.org/10.1007/s40544-017-0172-8

[42] Li Y, Yin X, Wu W. Preparation of Few-Layer MoS_2 Nanosheets via an Efficient Shearing Exfoliation Method. Ind Eng Chem Res. 2018; 57: 2838-2846.

[43] Yu H, Zhu H, Dargusch M, et al. A reliable and highly efficient exfoliation method for water-dispersible MoS_2 nanosheet. J Colloid Interface Sci. 2018; 514: 642-647.

[44] Xu L, Gu Y, Li Y, et al. One-step preparation of molybdenum disulfide/graphene nano-catalysts through a simple co-exfoliation method for high-performance electrocatalytic hydrogen evolution reaction. J Colloid Interface Sci. 2019; 542: 355-362.

[45] Dalila RN, Md Arshad MK, Gopinath SCB, et al. Current and future envision on developing biosensors aided by 2D molybdenum disulfide (MoS_2) productions. Biosens Bioelectron. 2019; 132: 248-264.

[46] Qiao S, Cong R, Liu J, et al. Vertical layered MoS_2/Si heterojunction for ultrahigh and ultrafast photoresponse photodetector. J Mater Chem C. 2018; 6: 3233-3239.

[47] Pak S, Jang AR, Lee J, et al. Surface functionalization-induced photoresponse characteristics of monolayer MoS_2 for fast flexible photodetectors. Nanoscale. 2019. https://doi.org/10.1039/C8NR07655C

[48] Zhang Y, Yu Y, Mi L, et al. In Situ Fabrication of Vertical Multilayered MoS_2/Si Homotype Heterojunction for High-Speed Visible-Near-Infrared Photodetectors. Small. 2016; 12: 1062-1071.

[49] Ye L, Li H, Chen Z, et al. Near-Infrared Photodetector Based on MoS_2/Black Phosphorus Heterojunction. ACS Photonics. 2016; 3: 692-699.

[50] Jia C, Wu D, Wu E, et al. A self-powered high-performance photodetector based on a MoS_2/GaAs heterojunction with high polarization sensitivity. J Mater Chem C. 2019; 7.

[51] Tsai D, Liu K, Lien D, et al. Few-Layer MoS_2 with High Broadband Photogain and Fast Optical Switching for Use in Harsh Environments. Acs nano. 2013; 7: 3905-3911.

[52] Zhang C, Nakano K, Nakamura M, et al. Noncentrosymmetric Columnar Liquid Crystals with the Bulk Photovoltaic Effect for Organic Photodetectors. J Am Chem Soc. 2020; 142: 3326-3330.

[53] Huang X, Mei C, Hu J, et al. Potential Superiority of p-Type Silicon-Based Metal-Oxide-Semiconductor Structures Over n-Type for Lateral Photovoltaic Effects. IEEE Electron Device Lett. 2016; 37: 1018-1021.

[54] Qi J, Ma N, Yang Y, Photovoltaic-Pyroelectric Coupled Effect Induced Electricity for Self-Powered Photodetector System. Adv Mater Interfaces. 2017; 29: 1701189.

[55] Li H, Li X, Park JH, et al. Restoring the Photovoltaic Effect in Graphene-based van der Waals Heterojunctions towards Self-Powered High-Detectivity Photodetectors. Nano Energy. 2019; 57: 214-221.

[56] Mech RK, Mohta N, Chatterjee A, et al. High Responsivity and Photovoltaic Effect Based on Vertical Transport in Multilaye α-In_2Se_3. Phys Status Solidi A. 2020; 217: 1900932.

[57] Buscema M, Island JO, Groenendijk DJ, et al. Photocurrent generation with two-dimensional van der Waals semiconductors. Chem Soc Rev. 2015; 44: 3691-3718.

[58] Shaygan M, Davami K, Kheirabi N, et al. Single-crystalline CdTe nanowire field effect transistors as nanowire-based photodetector. Phys Chem Chem Phys. 2014; 16: 22687-22693.

[59] Shinde SS, Rajpure KY. Fabrication and performance of N-doped ZnO UV photoconductive detector. J Alloys Compd. 2012; 522: 118-122.

[60] Li J, Yan X, Sun F, et al. Anomalous photoconductive behavior of a single InAs nanowire photodetector. Appl Phys Lett. 2015; 107: 263103.

[61] Su W, Weng W, Wang Y, et al. Mo_{1-x} W_xS_2-based photodetector fabrication and photoconductive characteristics. Jpn J Appl Phys. 2017; 56: 032201.

[62] Wang P, Liu Y, Yin J, et al. A tunable positive and negative photoconductive photodetector based on a gold/graphene/p-type silicon heterojunction. J Mater Chem C. 2019; 7: 887-896.

[63] Yang Z, Jiang B, Zhang Z, et al. The photovoltaic and photoconductive photodetector based on GeSe/2D semiconductor van der Waals heterostructure. Appl Phys Lett. 2020; 116: 141101.

[64] Saenz GA, Karapetrov G, Curtis J, et al. Ultra-high Photoresponsivity in Suspended Metal-Semiconductor-Metal Mesoscopic Multilayer MoS_2 Broadband Detector from UV-to-IR with Low Schottky Barrier Contacts. Sci Rep. 2018; 8: 1276-1286.

[65] Qin F, Gao F, Dai M, et al. Multilayer InSe-Te van der Waals heterostructures with ultrahigh rectification ratio and ultrasensitive photoresponse. ACS Appl Mater Interfaces. 2020; 12: 37313-37319.

[66] Lu X, Jiang P, Bao X. Phonon-enhanced photothermoelectric effect in $SrTiO_3$ ultra-broadband photodetector. Nat Commun. 2019; 10.

[67] Gosciniak J, Rasras M, Khurgin J. Ultrafast Plasmonic graphene photodetector based on channel photo-thermoelectric effect. ACS Photonics. 2020; 7: 488-498.

[68] He X, Wang X, Nanot S, et al. Photothermoelectric p-n Junction Photodetector with Intrinsic Broadband Polarimetry Based on Macroscopic Carbon Nanotube Films. Acs Nano. 2013; 7: 7271-7277.

[69] Kallatt S, Umesh G, Bhat N, et al. Photoresponse of atomically thin MoS_2 layers and their planar heterojunctions. Nanoscale. 2016; 8: 15213-15222.

[70] Liu J, Zhou Y, Lin Y, et al. Anisotropic Photoresponse of the Ultrathin GeSe Nanoplates Grown by Rapid Physical Vapor Deposition. ACS Appl Mater Interfaces. 2019; 11: 4123-4130.

[71] Sarwat SG, Youngblood N, Au YY, et al. Engineering Interface-Dependent Photoconductivity in $Ge_2Sb_2Te_5$ Nanoscale Devices. ACS Appl Mater Interfaces. 2018; https://doi.org/10.1021/acsami.8b17602

[72] Guo W, Dong Z, Xu Y, et al. Sensitive Terahertz Detection and Imaging Driven by the Photothermoelectric Effect in Ultrashort−Channel Black Phosphorus Devices. Adv Sci. 2020; 7: 1902699.

[73] Ra H S, Kwak DH, Lee JS. A hybrid MoS_2 nanosheet-CdSe nanocrystal phototransistor with a fast photoresponse. Nanoscale. 2016; 8: 17223-17230.

[74] Kufer D, Nikitskiy I, Lasanta T, et al. Hybrid 2D-0D MoS_2-PbS Quantum Dot Photodetectors. Adv Mater. 2015; 27: 176-180.

[75] Yang Y, Huo N, Li J. Sensitized monolayer MoS_2 phototransistors with ultrahigh responsivity. J Mater Chem C. 2017; 5: 11614-11619.

[76] Long M, Wang P, Fang H, et al. Progress, Challenges, and Opportunities for 2D Material Based Photodetectors. Adv Funct Mater. 2018; 1803807.

[77] Xu Z, Lin S, Li X, et al. Monolayer MoS_2/GaAs heterostructure self-driven photodetector with extremely high detectivity. Nano Energy. 2016; 23: 89-96.

[78] Li G, Li Z, Chen J, et al. Self-powered, high-speed Sb_2Se_3/Si heterojunction photodetector with close spaced sublimation processed Sb_2 Se_3 layer. J Alloys Compd. 2017; 737: 67-73.

[79] Huang R, Zhang J, Wei F, et al. Ultrahigh responsivity of ternary Sb-Bi-Se nanowire photodetectors. Adv Funct Mater. 2014; 24: 3581-3586.

[80] Kan H, Zheng W, Lin R, et al. Ultrafast Photovoltaic-Type Deep Ultraviolet Photodetectors Using Hybrid Zero-/Two-Dimensional Heterojunctions. ACS Appl Mater Interfaces. 2019; 11: 8412-8418.

[81] Liu S, Li M, Su D, et al. Broad-Band High-Sensitivity ZnO Colloidal Quantum Dots/Self-Assembled Au Nanoantennas Heterostructures Photodetectors. ACS Appl Mater Interfaces. 2018; 10: 32516-32525.

[82] Ma S, Li K, Xu H, et al. A Lattice-mismatched PbTe/ZnTe Heterostructure with High-speed Mid-infrared Photoresponses. ACS Appl Mater Interfaces. 2019; https://doi.org/10.1021/acsami.9b13154

[83] Li L, Lou Z, Chen H, et al. Stretchable SnO_2-CdS interlaced-nanowire film ultraviolet photodetectors. Sci China Mater. 2019; https://doi.org/10.1007/s40843-019-9416-7

[84] Nazir G, Khan MF, Akhtar I, et al. Enhanced photoresponse of ZnO quantum dot-decorated MoS_2 thin films. RSC Adv. 2017; 7: 16890-16900.

[85] Xu H, Wu J, Feng Q, et al. High responsivity and gate tunable graphene-MoS_2 hybrid phototransistor. Small. 2014; 10: 2300-2306.

[86] Long M, Gao A, Wang P, et al. Room temperature high-detectivity mid-infrared photodetectors based on black arsenic phosphorus. Sci Adv. 2017; 3: e1700589.

[87] Zhang Y, Yu Y, Wang X, et al. Solution assembly MoS_2 nanopetals/GaAs n–n homotype heterojunction with ultrafast and low noise photoresponse using graphene as carrier collector. J Mater Chem C. 2016; 5: 140-148.

[88] Zhuo R, Wu D, Wang Y, et al. A self-powered solar-blind photodetector based on a MoS_2/β-Ga_2O_3 heterojunction. J Mater Chem C. 2018; 6.

[89] Ahn J, Kang JH, Kyhm JH et al. Self-Powered Visible-Invisible Multiband Detection and Imaging Achieved Using High-Performance 2D $MoTe_2$/MoS_2 Semivertical Heterojunction Photodiodes. ACS Appl Mater Interfaces. 2020; 12: 10858-10866.

[90] Yu Y, Li Z, Lu Z, et al. Graphene/MoS_2/Si Nanowires Schottky-NP Bipolar van der Waals Heterojunction for Ultrafast Photodetectors. IEEE Electron Device Lett. 2018; 39.

[91] Xue Y, Zhang Y, Liu Y, et al. Scalable Production of a Few-Layer MoS_2/WS_2 Vertical Heterojunction Array and Its Application for Photodetectors. Acs Nano. 2016; 10: 573-580.

[92] Wang L, Jie J, Shao Z, et al. MoS_2/Si Heterojunction with Vertically Standing Layered Structure for Ultrafast, High−Detectivity, Self−Driven Visible-Near Infrared Photodetectors. Adv Funct Mater. 2015; 25: 2910-2919.